Journal of
Ceramic Science
and Technology

J. Ceram. Sci. Tech., 02 [04] 203-210 (2011)
DOI: 10.4416/JCST2011-00021
available online at: http://www.ceramic-science.com

Synthesis and Characterization of Mesoporous Sodium Dodecyl Sulfate-Coated Magnetite Nanoparticles

R. El-kharrag[1], A. Amin[1], Y. E. Greish*[2]

[1]Department of Biology, and
[2]Department of Chemistry College of Science, United Arab Emirates University, Al Ain, P.O. Box 17551, UAE

received July 2, 2011; received in revised form August 1, 2011; accepted August 16, 2011

Abstract

Mesoporous magnetite nanoparticles are commonly used for biomedical and environmental applications. This can be attributed to their known magnetic properties and high surface area, the latter being a virtue of their nanometer-scale size. Applying coatings with various chemical functionalities to these nanoparticles increases their scope of application. Different organic and inorganic coatings have been explored. Sodium dodecyl sulfate (SDS) is a well-known surfactant that improves the surface properties of nanoparticles. This paper explores the *in situ* formation of SDS coatings on the surface of mesoporous magnetite nanoparticles prepared by means of a traditional co-precipitation method in air. Coatings made from solutions containing up to 2 wt% of SDS were investigated in respect of their composition, thermal characteristics, and magnetization by means of X-ray diffraction, infrared spectroscopy, thermogravimetric analysis and magnetic susceptibility. Adsorption isotherms and detailed morphology of the coated nanoparticles were also evaluated. Results showed that SDS forms multilayers together with water on the surfaces of the nanoparticles, where a maximum initial concentration of 0.5 wt% of SDS could be used to homogeneously coat the magnetite nanoparticles. At higher concentrations, SDS detaches from the nanoparticles surfaces.

Keywords: Magnetite nanoparticles, mesoporous, sodium dodecyl sulfate, thermal analysis, magnetic susceptibility

I. Introduction

Iron oxide nanoparticles, especially magnetite (Fe_3O_4) nanoparticles, have been extensively studied for various applications [1–5]. Their known magnetic properties have strongly recommended them for biomedical and environmental applications. Magnetite nanoparticles have been used in biomedical applications such as drug delivery [6] and as MRI contrast agents [7]. On the other hand, they have also been used as adsorbents for the removal of soluble heavy metal cations and organic pollutants from waste water [8]. In both types of applications, researchers make use of the two main attributes of magnetite nanoparticles: their magnetic properties and their high surface area derived from their nanometer scale. In addition, mesoporosity created in aggregates of nanoparticles has led to their use as catalysts and sensors for various organic reactions [9].

Magnetite nanoparticles with pre-tailored chemical functionalities have also been found to increase the scope of applications of magnetite nanoparticles. Various organic and inorganic coatings have been investigated in this regard [10–13]. The choice of coating is application-driven. For example, for biomedical applications, having a biocompatible coating is a major concern [14]. In addition, if these coated nanoparticles are to be used to deliver certain bioactive drugs into infection or tumor sites, the chemical characteristics of the coating should match those of the bioactive drugs to ensure bonding between them until delivery takes place [15–18]. Similarly, the presence of organic coatings such as chitosan [19] and sodium dodecyl sulfate [20] have been shown to enhance the ability of magnetite nanoparticles to remove pollutants from waste water. This is attributed to the binding and chelating efficiency of the functional groups in these coatings. In both types of applications, maintaining a narrow particle size distribution is another major requirement. To achieve this, various methods of preparation have been investigated [14]. Synthesis of magnetite nanoparticles in the presence of organic molecules – simple or polymeric – has been found to be effective in reducing the particle size of the prepared nanoparticles [21–23]. Maintaining an O_2-free atmosphere has also been extensively applied to avoid oxidation of the prepared magnetite nanoparticles [14,24–26]. In our previous article, we showed that monolithic magnetite nanoparticles can be prepared with a simple co-precipitation procedure in air [27]. To maintain the purity of the prepared nanoparticles, starting materials were added to a strongly basic solution to ensure the formation of magnetite as the most thermodynamically stable phase [28].

The role of SDS in stabilizing different types of nanoparticles has been previously studied [29]. Shariati *et al.* and Keyhanian *et al.* explored the use of magnetite nanoparticles modified with SDS for the removal of Safranin O and methyl violet dyes from aqueous media [20,30]. In their

* Corresponding author: y.afifi@uaeu.ac.ae

work, SDS was added to ready-made magnetite nanoparticles. Faraji *et al.* studied the application of SDS-coated magnetite for the removal of trace amounts of mercury from waste water [31]. Zheng *et al.* used SDS in combination with oleic acid to form magnetite aggregates that were further coated with styrene monomer and then *in situ* [32]. The current study investigates the synthesis of mesoporous magnetite nanoparticles by means of co-precipitation in the presence of various concentrations of SDS. The formed magnetite nanoparticles as well as the SDS-coated nanoparticles were characterized with XRD, FT-IR, TGA, SEM, TEM, and magnetic susceptibility measurements at room temperature.

II. Materials and Methods

In the current study, magnetite nanoparticles were prepared with a slightly modified co-precipitation method. The entire process was conducted in air. Chemicals used included iron (II) chloride tetrahydrate ($FeCl_2{\cdot}4H_2O$), iron (III) chloride ($FeCl_3$), sodium hydroxide (NaOH) and ammonia solution (NH_4OH), and sodium dodecyl sulfate (SDS). All reagents were analytical-grade and purchased from Sigma-Aldrich, USA. Aqueous solutions containing 0.3 *M* of Fe^{2+} and 0.6 *M* of Fe^{3+} were separately prepared by dissolving the respective amounts of $FeCl_2{\cdot}4H_2O$ and $FeCl_3$ in de-ionized water. An aqueous solution of NaOH of pH 13 was also prepared by dissolving the corresponding amount of NaOH in de-ionized water. A pre-calculated volume of the NaOH solution was heated to 60 °C in a round flask. A mixture containing equal volumes of Fe^{2+} and Fe^{3+} was injected into the NaOH solution at feeding rates of 40 mL/h with vigorous stirring. At the end of the addition, a brownish-black precipitate was formed. The whole solution was vigorously stirred at the same constant temperature for 60 min. Magnetite suspensions were then soaked at 60 °C for 24 h without stirring. The magnetite suspensions were then centrifuged at 3000 rpm for 15 min followed by successive decantation/washing with 25 % ammonia solution three times. After the final decantation, the magnetite deposits were collected and dried at 60 °C for 24 h. The dried powders were finely ground to be characterized in respect of their composition, morphology, surface area, and magnetic susceptibility.

To prepare SDS-coated magnetite nanoparticles, the same process as described above was repeated with the SDS being initially dissolved in water at a pre-defined concentration then added to the NaOH solution prior to injection of the Fe^{2+}/Fe^{3+} solution. Initial concentrations of SDS investigated were 0.2, 0.5, 1.0 and 2.0 % by weight of the original Fe^{2+}/Fe^{3+} reactants.

Composition of the prepared magnetite was studied by means of X-ray diffraction and infrared spectroscopy. An automated x-ray diffractometer with a step size of 0.02°, scan rate of 2 ° per min, and a scan range from $2\theta = 10$ ° to 70 ° was used. FT-IR analysis was conducted with a Nicolet Nexus 470 infrared spectrophotometer, USA, where samples were pre-pressed with KBr, and scanned over the normal range of 4000 – 400 cm^{-1}. The microstructures of solid magnetite samples were evaluated with a JEOL SEM at an accelerating voltage of 15 kV. A detailed description of the morphology of the nanoparticles was obtained by means of transmission electron microscopy (TEM), CM1 – Philips Transmission Electron Microscope, Netherlands. Thermogravimetric analysis (TGA) was also applied to investigate the thermal properties of the prepared nanoparticles with a TGA-50 Shimadzu thermogravimetric analyzer where pre-weighed powder samples were heated to 600 °C at a heating rate of 20 °C/min. BET surface area, porosity, pore size distribution and pore volume of the dried solid samples were measured by means of nitrogen gas adsorption at 77 K with a Quantochrome NOVA 1000 volumetric gas sorption instrument, Autosorb, USA. Magnetic susceptibility measurements were performed at room temperature with a magnetic susceptibility balance (MSB-Auto, Sherwood Scientific Ltd, England). A pre-determined mass of finely ground magnetite nanoparticles was filled into a narrow glass tube and subjected to a magnetic field (4.5 kGauss). The data were expressed as mass susceptibility (χ_g) in m^3/kg.

III. Results and Discussion

Magnetite nanoparticles were prepared in the current study with a simple co-precipitation procedure in which Fe^{2+} and Fe^{3+} ions were co-added in air to a highly basic medium with a pH of 13. Electrochemical studies revealed that magnetite is the most thermodynamically stable phase that will deposit under these conditions [28]. In a previous article, this was proven to be the case although all preparations were performed in air in which a possibility of oxidation of Fe^{2+} to Fe^{3+} was always considered [27]. Fig. 1 shows the XRD pattern of magnetite nanoparticles formed under the above-mentioned conditions. A standard XRD pattern of pure magnetite (JCPDS card # 89 – 0691) is also shown for comparison. Peaks characteristic of magnetite at 2θ values of 29.9 ° (220), 35.2 ° (311), 43.1 ° (400), 53.4 ° (422), 57.1 ° (511), and 62.8 ° (440) were observed, indicating the high crystallinity and phase purity of the prepared magnetite. Despite the high pH of the medium in which magnetite was precipitated, electrostatic stabilization did not take place. As a result, nanoparticles were clustered in the form of round-shape aggregates (Fig. 2a), with

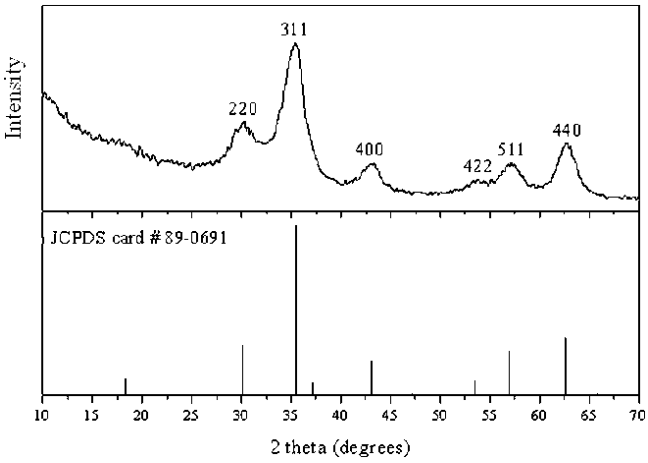

Fig. 1: X-ray diffraction pattern of magnetite nanoparticles prepared with a co-precipitation method involving Fe^{2+} and Fe^{3+} ions in a highly basic medium.

an average size of 220 nm (Fig. 2b). These aggregates were mesoporous in nature as was observed in N_2-adsorption studies. Fig. 3a shows an adsorption-desorption isotherm of magnetite aggregates prepared in the current study. The hysteresis loops in Fig. 3a are of type IV where the lower curve represents the adsorption of N_2 gas on the surfaces of the nanoparticles, while the upper curve represents the progressive withdrawal, that is desorption, of the adsorbed N_2 gas [33]. Based on the isotherms in Fig. 3a, pore volume distributions were calculated in all powders samples and were plotted in Fig. 3b. A homogeneous pore size distribution with a maximum of 30 – 40 nm was observed. This range denotes the presence of mesoporosity in the agglomerates of the prepared nanoparticles [33]. The monodispersity in the pore size distribution within the agglomerates relatively reflects the homogeneity of the particle size distribution in these samples. Mesoporosity in agglomerates composed of nanoparticles is considered an important requirement if they are to be used as adsorbents and catalysts for various chemical reactions with potential environmental importance [34].

Fig. 4 shows infrared spectra of magnetite nanoparticles coated with various concentrations of SDS. The FT-IR spectrum of pure SDS is also shown for comparison. Magnetite phase is characterized by its main band at 429.6 – 441.9 cm^{-1}. On the other hand, the sulfate group in SDS is characterized by its bands at 998.5, 1019.3 and 1082.2 cm^{-1} for its symmetric absorption, and at 1223.1 and 1248.9 cm^{-1} for its asymmetric absorption [29]. Location and shape/sharpness of these bands in the FT-IR spectra of SDS-coated magnetite samples changed as a result of the interaction between the SDS coating and the underlying magnetite nanoparticles. Details of these changes are given in Table 1. Positions of the pure SDS bands are related to the symmetric and asymmetric absorption of $-OSO_3^-$ in the $-OSO_3Na$ group of SDS. Changes in the band position of the corresponding bands in SDS-coated magnetite are attributed to the formation of bonds between the sulfate group and the Fe^{2+} and Fe^{3+} ions in the underlying magnetite nanoparticles, which is similar to the previous findings on comparable oxides [29]. This shift was shown to increase with an increasing concentration of SDS. This observation was more evident in the

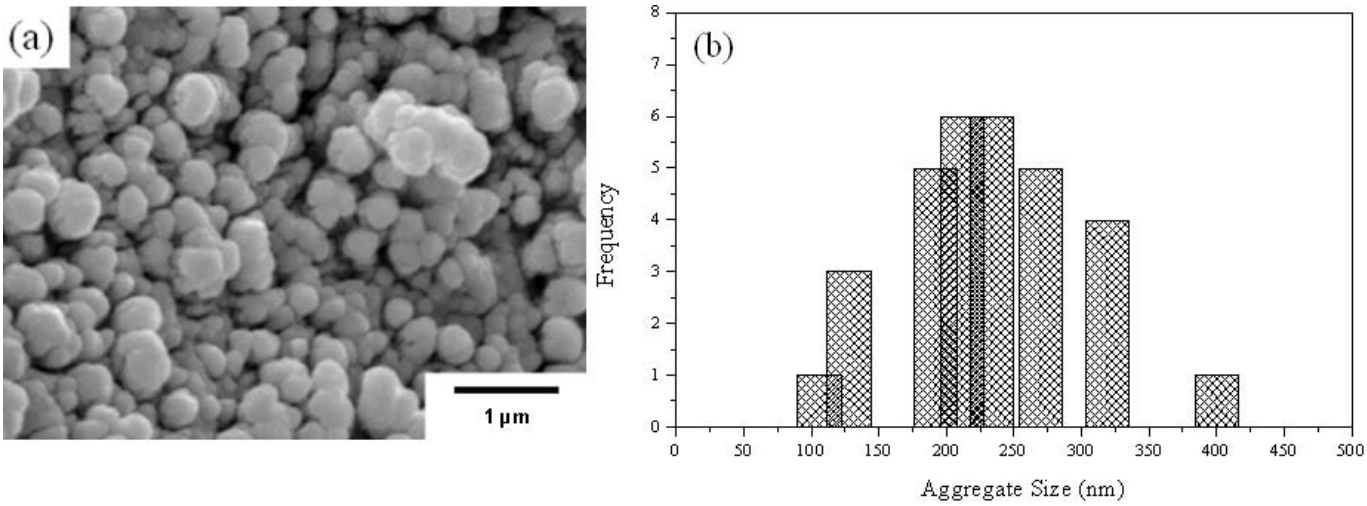

Fig. 2: a) Scanning electron micrograph, and b) size distribution of magnetite aggregates prepared with a co-precipitation method involving Fe^{2+} and Fe^{3+} ions in a highly basic medium.

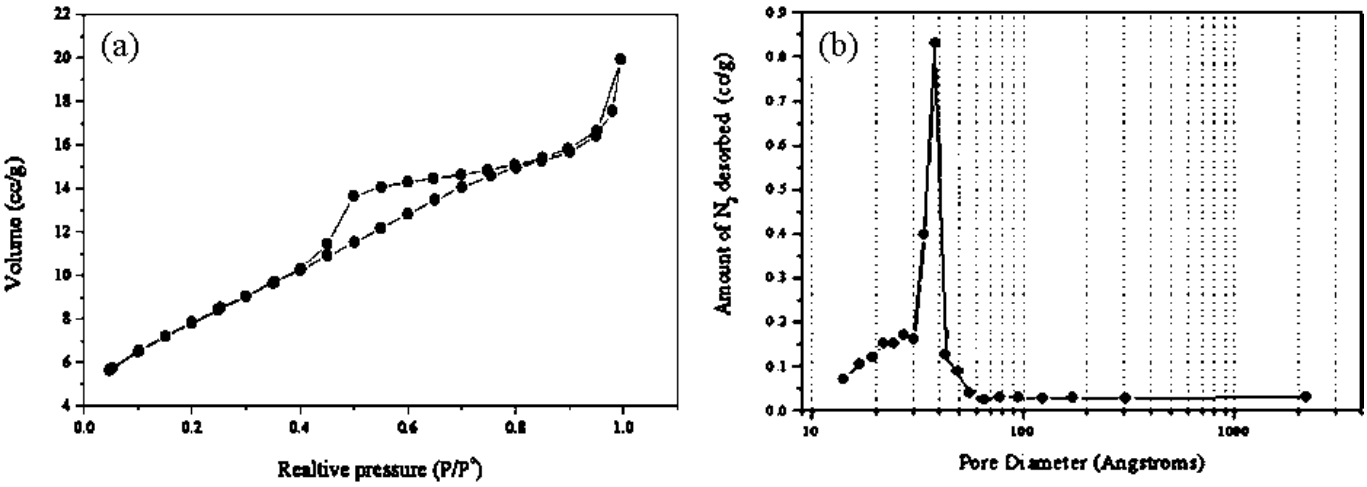

Fig. 3: a) Adsorption isotherm, and b) pore size distribution of magnetite aggregates prepared with a co-precipitation method involving Fe^{2+} and Fe^{3+} ions in a highly basic medium.

FT-IR spectra of SDS-coated magnetite samples containing 1.0 and 2.0 wt% of SDS. It should be mentioned that un-adsorbed SDS was removed from all samples by washing, which confirms that the observed bands are solely related to SDS coatings.

Table 1: Wave number of the absorption bands characteristic of the sulfate group in SDS as appeared in pure SDS and SDS-coated magnetite FT-IR spectra

	ν_s (-OSO_3^-)			ν_{as} (-OSO_3^-)	
SDS	998.5	1019.3	1082.2	1223.1	1248.9
0.2 %	1010.2		***	***	
0.5 %	1005.3		***	1247.6	
1.0 %	969.2		1062.8	1242.1	
2.0 %	957.8		1062.8	1229.9	

*** bands were not observed in the FT-IR spectra of these samples

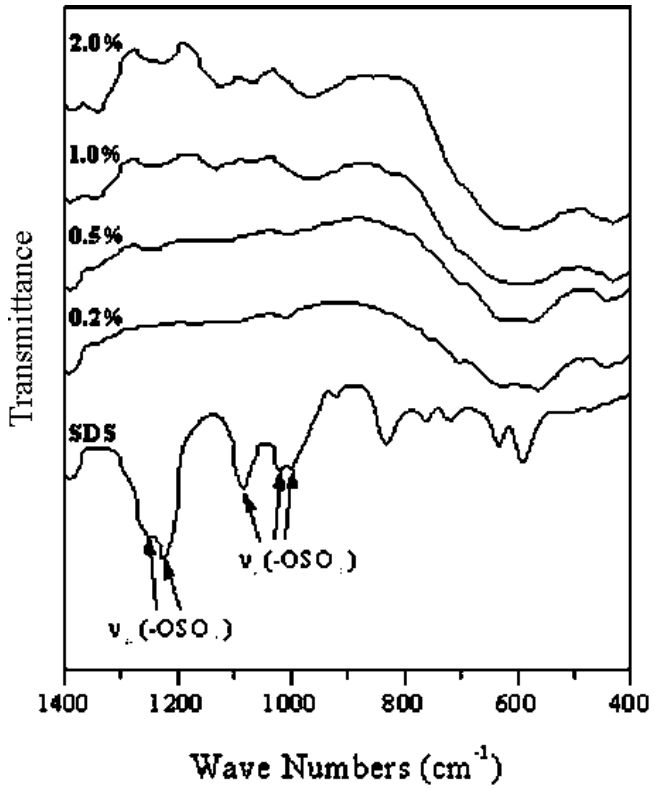

Fig. 4: Infrared spectra of pure magnetite and magnetite coated with various concentrations of SDS.

Fig. 5 shows the TGA analysis of SDS-coated magnetite nanoparticles. TGA curves of pure magnetite and SDS are also shown for comparison. SDS starts losing weight in a single step at a temperature of 180 °C, which denotes its degradation. This process increases until it levels off at a temperature of 470 °C with an overall weight loss of 75.3 % where SDS was completely degraded. On the contrary, pure magnetite shows an overall weight loss of 14 % and starts at a temperature of slightly below 100 °C and continues in a single step with a sharp decrease until 115 °C, after which a slow decrease in the rate of weight loss takes place. This weight loss is attributed to the removal of physically and chemically attached water. The continued weight loss reflects the presence of multiple layers of water attached to the magnetite nanoparticles, which are initially negatively charged owing to the high pH of the medium in which they were prepared. SDS-coated magnetite nanoparticles showed variable degrees of weight loss, which is related to the concentration of SDS initially used during the synthesis process. All SDS-coated nanoparticles showed two steps of weight loss; an initial step that started at a temperature slightly below 100 °C, and a second step that started at a temperature close to 200 °C. The first step is related to the evaporation of physically and chemically attached water, while the second step is related to the degradation of the SDS coating the nanoparticles. These results confirm the presence of SDS as a coating on the surface of the prepared nanoparticles, as was previously shown in the IR spectra of these samples (Fig. 4). These findings also confirm the presence

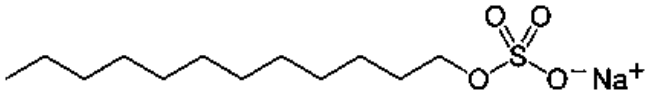

Scheme 1: Structure of Sodium Dodecyl Sulfate (SDS).

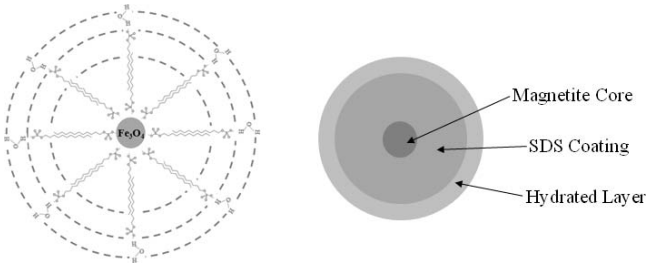

Scheme 2: Interaction between SDS and surface of magnetite nanoparticles.

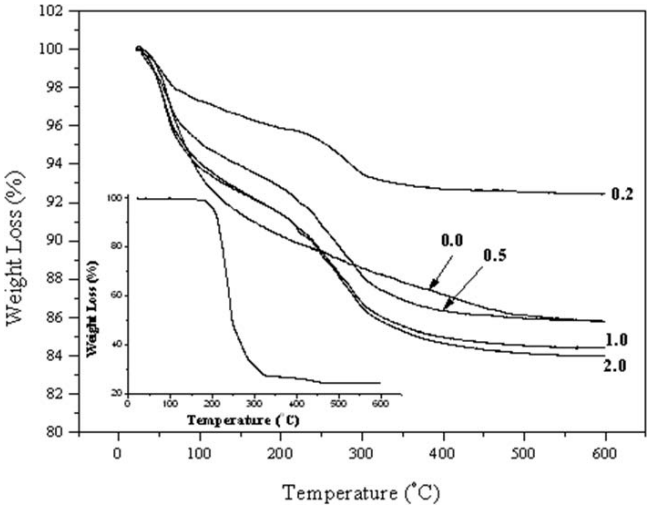

Fig. 5: Thermogravimetric analysis of magnetite coated with various concentrations of SDS. Insert: TGA pattern of pure SDS.

of multi-layers of SDS coating the nanoparticles on which water was adsorbed. This explains the removal of water as an initial step followed by the removal of the underlying SDS layer, as shown in Scheme 2. Detailed analysis of the contribution of water and SDS in the overall weight

loss observed for all SDS-coated magnetite nanoparticles is shown in Fig. 6. In the absence of SDS, i.e. in pure mag-

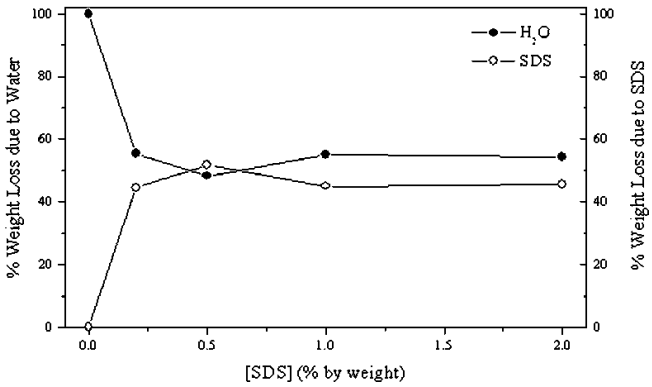

Fig. 6: Analysis of the TGA curves of magnetite and SDS-coated magnetite nanoparticles shown in Fig. 5

netite, the weight loss is related to water only. As the concentration of SDS in solution was increased, a pronounced decrease in the weight loss owing to water was observed and a consequent increase in the weight loss owing to the SDS was observed. This behavior continued up to 0.5 wt% of SDS. As the percentage of SDS was increased to 1 %, its contribution to the overall weight loss was decreased with a subsequent increase in the contribution of water to the overall weight loss. The same criterion was also observed when 2 wt% of SDS was initially added. These results suggest that at SDS percentages above 0.5 %, its molecules detach from the coating and are replaced by water. Detachment of adsorbed molecules takes place when these molecules are weakly bonded to the substrate, i.e. the magnetite nanoparticles. This indicates that the desorbed molecules are in the outermost layer of SDS coating the nanoparticles. Primary layers are thermodynamically known to strongly bond to the underlying substrate, whereas this bonding decreases in strength for molecules in the external layers of the coating [35]. This is attributed to the weaker intermolecular bonding between the SDS molecules compared to the direct ionic bonding between the SDS molecules in the primary layer and the underlying magnetite nanoparticles, as represented in Scheme 2. These findings, therefore, indicate that the highest SDS content in the coating is achieved when its initial concentration is 0.5 wt%.

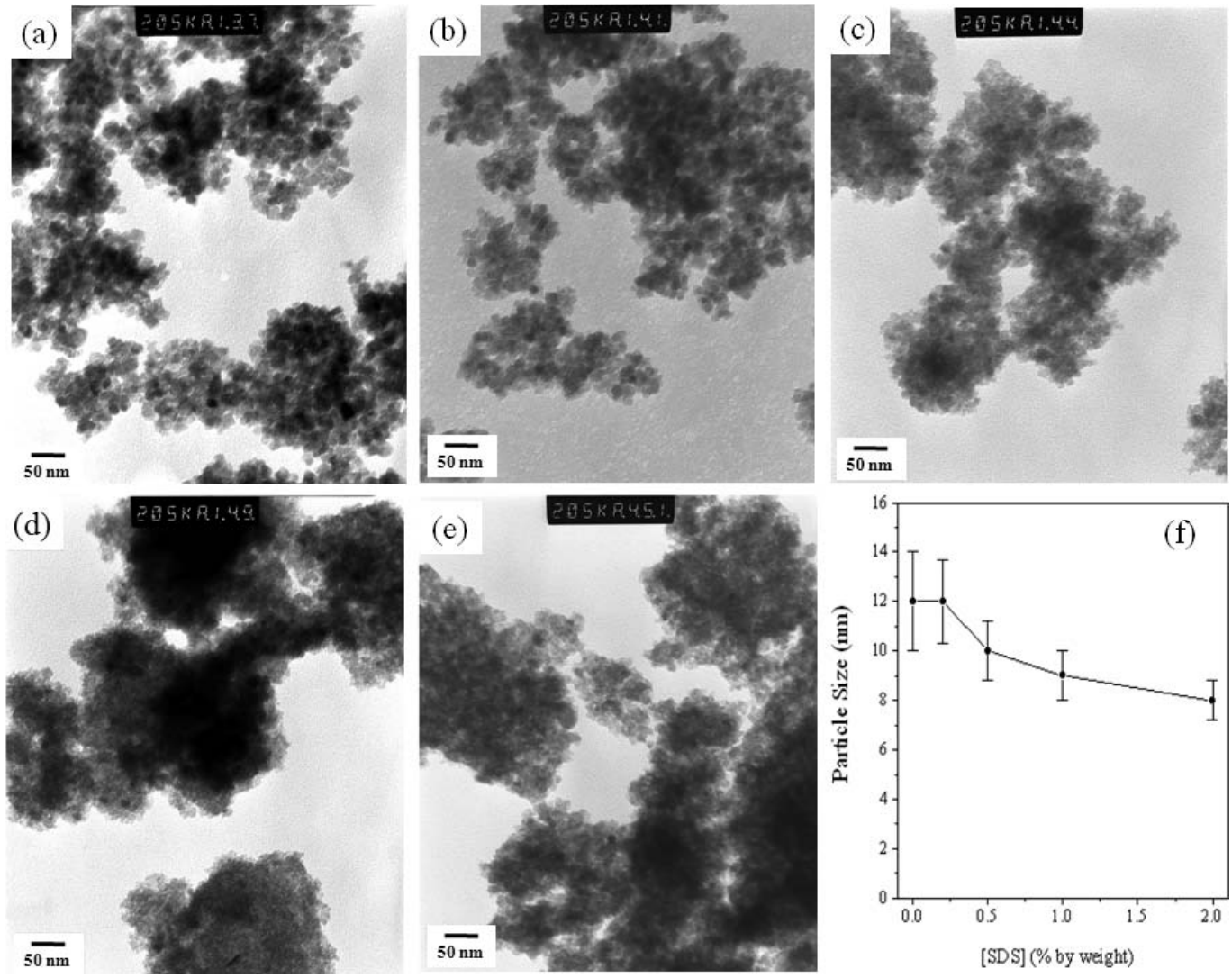

Fig. 7: Transmission electron micrographs of neat and SDS-coated magnetite nanoparticles containing. a) 0 %, b) 0.2 %, c) 0.5 %, d) 1.0 %, and e) 2.0 % SDS by weight. e) average particle size distribution of neat and SDS-coated magnetite nanoparticles.

Transmission electron micrographs of neat and SDS-coated magnetite nanoparticles in Fig. 7 show the detailed microstructures of these powders. The magnetite nanoparticles shown in Fig. 7a are uniform in size and spherical in shape with an average particle size of 12 nm. The addition of a low concentration of 0.2 wt% of SDS did not affect the particles' morphology or their size. Increasing the concentration of SDS caused a systematic decrease of the particle size, achieving 8 nm in presence of 2 wt% of SDS, Fig. 7f. This was the smallest size achieved in the presence of SDS. These results suggest the effect of SDS as a capping agent that limits the size of magnetite nuclei formed during precipitation in the aqueous medium. It is also evident that the size of particles could be controlled by adjusting the amount of SDS added. The presence of SDS on the surface of magnetite nanoparticles was also confirmed by EDX analysis, as shown in Fig. 8, which compares the elemental analysis of neat magnetite nanoparticles and those coated with 1 wt% SDS. A peak characteristic of the X-ray K_a line of S, of the sulfate functional group of SDS, was observed on the coating, while the spectrum of neat magnetite only showed the presence of iron as the main element. The decrease in particle size as a result of the addition of SDS was reflected in an increase in the surface area of the formed nanoparticles, as shown in Fig. 9a. A pronounced increase

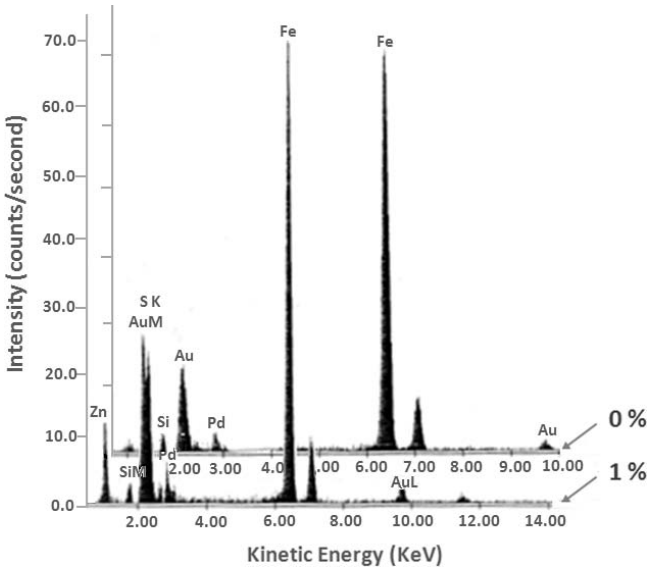

Fig. 8: Energy-dispersive X-ray spectra of neat magnetite and magnetite nanoparticles coated with 1 wt% SDS (y-axis represents intensity of the peaks).

in the surface area from 139 m^2/g for neat magnetite to 189 m^2/g of nanoparticles formed in the presence of 2 wt% of SDS was observed. A comparison between the decrease in the particle size with the increase in the concentration of SDS (Figs. 6 and 7f) indicates that a constant proportion of SDS would be adsorbed on the surface of magnetite

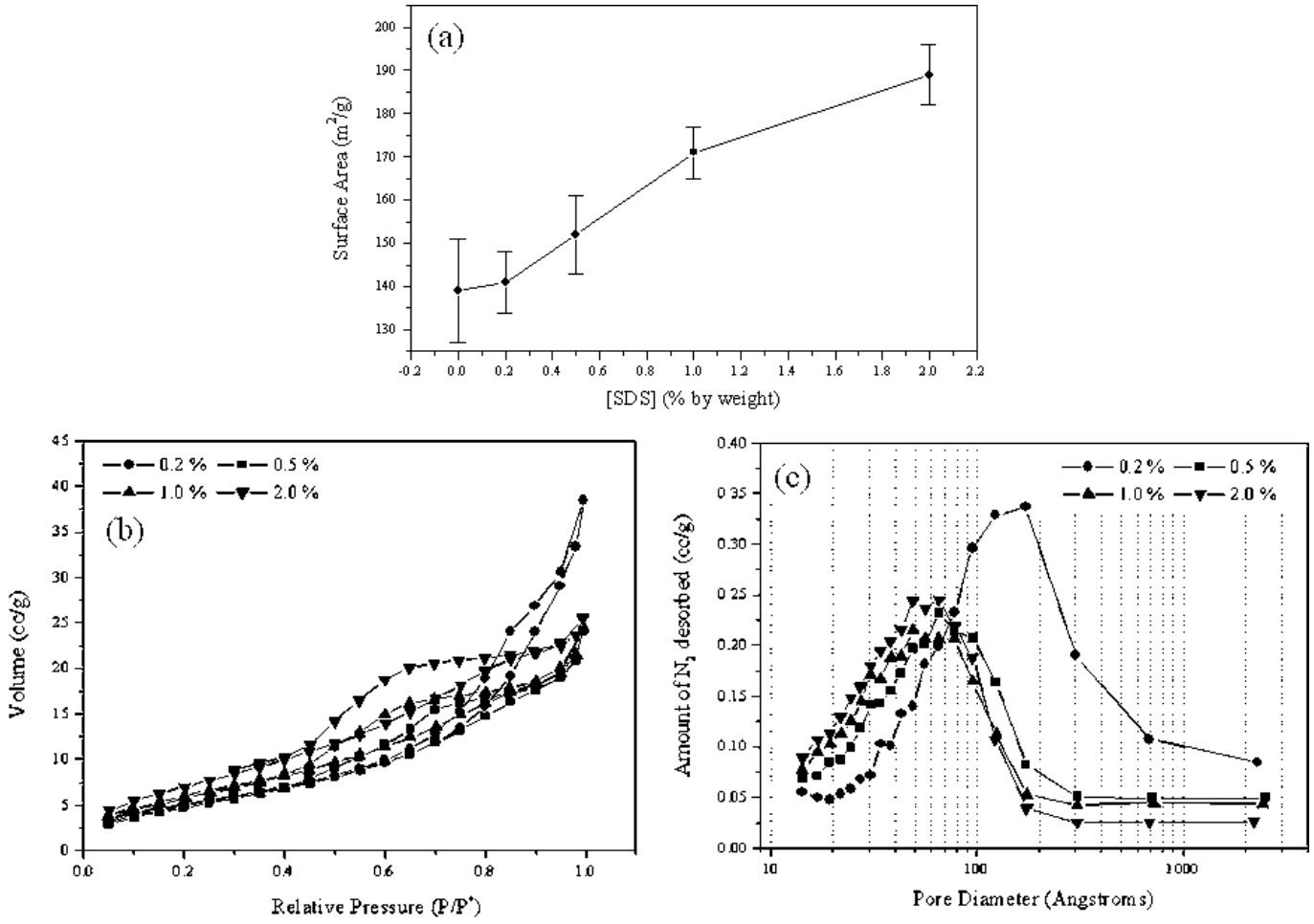

Fig. 9: a) Surface area, b) adsorption isotherms, and c) pore size distribution curves of SDS-coated magnetite aggregates.

nanoparticles regardless of the initial concentration of SDS used. The low particle size and high surface area of the SDS-coated magnetite nanoparticles strongly recommend them for biomedical applications, such as drug delivery, and for environmental applications as adsorbents for the removal of organic and inorganic pollutants from waste water. The latter suggested applications are also based on the fact that these nanoparticles form mesoporous aggregates with an average pore volume of 50 nm (Fig. 9b and c), which is in accordance with the low particle size of the nanoparticles forming these aggregates [33]. All aggregates showed hysteresis loops of type IV where the lower curve represents the adsorption of N_2 gas on the surfaces of the nanoparticles, while the upper curve represents the progressive withdrawal, i.e. desorption, of the adsorbed N_2 gas [33]. Aggregates of nanoparticles coated with 2 wt% SDS appear to have macroporosity with a larger pore volume of 150 nm, which is a reflection of the larger particle size of these particles. Comparing the results of Fig. 9b and c with those in Fig. 3 of the aggregates consisting of neat magnetite nanoparticles indicates that the mesoporosity of the neat magnetite aggregates is maintained even after coating with various concentrations of SDS.

Although both types of aggregates are mesoporous, the advantage of having SDS on the surface of magnetite nanoparticles is the presence of the functional group sulfate of the SDS coating. This enables SDS-coated magnetite nanoparticles to bind to organic pollutants in waste water and immobilize bioactive compounds to act as drug delivery vehicles, while the magnetite core makes their tracking more convenient than traditional adsorbents and drug delivery candidates. Magnetization of the SDS-coated magnetite nanoparticles was evaluated based on their magnetic susceptibility, as shown in Fig. 10. Magnetic susceptibility is the degree to which a material can be magnetized in an external magnetic field, and is directly proportional to the magnetization of the material based on the following relation [36]:

$$\mathbf{M} = \chi_{\upsilon}\, \mathbf{H}$$

where H is the magnetic field strength, which is normally kept constant during the susceptibility measurements. In addition, the magnetic size is known to be directly proportional to the magnetic susceptibility of solid nanoparticles [37]. A decrease in the susceptibility was observed when 0.2 wt% SDS was used to coat the magnetite nanoparticles. Despite the close similarity in particle size, this could be attributed to agglomeration of the nanoparticles caused by the hydrophilic interaction between them. The size of these aggregates was shown in Figs. 9 b and c to be larger than other types of aggregates in the current study [38]. This was implied from the higher pore volume in Fig. 9c. In the presence of 0.5 wt% of SDS, an increase in the magnetic susceptibility was observed, which could be attributed to the decrease in size of the SDS-coated nanoparticles, as shown in Fig. 7f, and the presence of a higher content of SDS in the coating compared to other types of SDS-coated nanoparticles, Fig. 6. An increase in the initial concentration of SDS, however, was reflected in a slight decrease in the susceptibility of the SDS-coated nanoparticles. Despite the decrease in size of these nanoparticles with the addition of SDS, their expected agglomeration could be used to explain the decrease in the susceptibility of these samples. Taken together, all SDS-coated nanoparticles showed variable degrees of magnetization that depend on the size of the nanoparticles and the concentration of SDS in the coating.

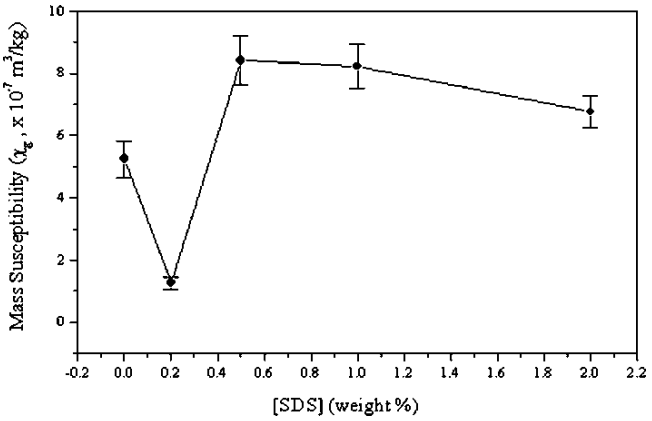

Fig. 10: Mass susceptibility of SDS-coated magnetite nanoparticles as a function of the weight percentage of SDS in the coating.

IV. Summary

The current study showed the possibility of formation of monolithic mesoporous magnetite nanoparticles that were further coated with SDS. The average particle sizes of the pure and coated magnetite nanoparticles were in the range of 8 – 12 nm. No indication of the presence of non-magnetite phases was found in the XRD pattern of the prepared nanoparticles. IR results indicated that SDS forms homogeneous coatings on the nanoparticles surfaces as a result of electrostatic attraction between the sulfate functional group of SDS and the underlying magnetite surfaces. Thermogravimetric studies showed that both water and SDS form multilayered coatings on the nanoparticles surfaces. A maximum of 0.5 wt% of SDS was proven sufficient to coat the nanoparticles surfaces. Both neat and coated nanoparticles form aggregates with mesoporosity and a maximum average pore volume of 50 nm. Variation of the magnetic susceptibility of the nanoparticles coated with SDS was attributed to the formation of aggregates and to their small particle size. The characteristics of the prepared neat and SDS-coated magnetite nanoparticles strongly recommend them for further investigation of their biomedical and environmental applications.

References:

1 Sun, S., Murray, C.B., Weller, D., Folks, L., Moser, A.: Monodisperse FePt nanoparticles and ferromagnetic FePt nanocrystal superlattices, *Science,* **287**, 1989 – 1992, (2000).

2 Jain, T.K., Morales, M.A., Sahoo, S.K., Leslie-Pelecky, D.L., Labhasetwar, V.: Iron oxide nanoparticles for sustained delivery of anticancer agents. *Mol. Pharm.*, **2**, 194 – 205, (2005).

3 Bulte, J.W.: Intracellular endosomal magnetic labeling of cells, *Methods Mol. Med.*, 124, 419 – 439, (2006).

4 Burtea, C., Laurent, S., Roch, A., Vander Elst, L., Muller, R.N.: C-MALISA (Cellular magnetic-linked immunosorbent assay), a new application of cellular ELISA for MRI, *J. Inorg. Biochem.*, **99**, 1135 – 1144, (2005).

5 Babes, L., Denizot, B., Tanguy, G., Le Jeune, J.J., Jallet, P.: Synthesis of iron oxide nanoparticles used as MRI con-

trast agents: A parametric study, *J. Colloid Interface Sci.*, **2**, 474 – 482, (1999).

6 Gupta, A.K., Gupta, M.: Synthesis and surface engineering of iron oxide nanoparticles for biomedical applications, *J. Biomater.,* **26**, 3995 – 4021, (2005).

7 Kim, E.H., Lee, H.S., Kwak, B.K., Kim, B.K.: Synthesis of ferrofluid with magnetic nanoparticles by sonochemical method for MRI contrast agent, *J. Magn. Magn. Mater.,* **289**, 328 – 330, (2005).

8 Mayo, J.T., Yavuz, C., Yean, S., Cong, L., Shipley, H., Yu, W., Falkner, J., Kan, A., Tomson, M., Colvin, V.: The effect of nanocrystalline magnetite size on arsenic removal, *Sci. Technol. Adv. Mater*., **8**, 71 – 75, (2007).

9 Lim, S., Woo, E., Lee, H., Lee, C.: Synthesis of magnetite-mesoporous silica composites as adsorbents for desulfurization from natural gas, *Appl. Cat. B: Env.,* **85**, 71 – 76, (2008).

10 Gupta, A.K., Wells, S.: Surface-modified superparamagnetic nanoparticles for drug delivery: Preparation, characterization, and cytotoxicity studies, *IEEE Trans. Nanobiosci.,* **3**, 66, (2004).

11 Tsai, Z.T., Wang, J.F., Kuo, H.Y., Shen, C.R., Wang, J.J., Yen, T.C.: *In situ* preparation of high relaxivity iron oxide nanoparticles by coating with chitosan: A potential MRI contrast agent useful for cell tracking, *J. Magn. Magn. Mater.*, **322**, 208 – 213, (2010).

12 Illés, E., Tombácz, E.: The role of variable surface charge and surface complexation in the adsorption of humic acid on magnetite, *J. Colloids Surf. A*., **230**, 99 – 109, (2003).

13 Zhang, X.L., Niu, H.Y., Zhang, S.X., Cai, Y.Q.; Preparation of a chitosan-coated C18-functionalized magnetite nanoparticle sorbent for extraction of phthalate ester compounds from environmental water samples, *J. Anal. Bioanal. Chem.,* **397**, 791 – 798, (2010).

14 Laurent, S., Forge, D., Port, M., Roch, A., Robic, C., Vander Elst, L., Muller, R.N.: Magnetic iron oxide nanoparticles: Synthesis, stabilization, vectorization, physicochemical characterizations, and biological applications, *J. Chem. Rev.,* **108**, 2064 – 2110, (2008).

15 Guo, S., Li, D., Zhang, L., Li, J., Wang, E.: Monodisperse mesoporous superparamagnetic single-crystal magnetite nanoparticles for drug delivery, *Biomater*., **30**, 1881 – 1889, (2009).

16 Gupta, A.K., Curtis, A.S.G.: Lactoferrin and ceruloplasmin derivatized superparamagnetic iron oxide nanoparticles for targeting cell surface receptors, *Biomater.*, **25**, 3029 – 3040, (2004).

17 Jain, T.K., Morales, M.A., Sahoo, S.K., Leslie, D.L., Labhasetwar, V.: Iron oxide nanoparticles for sustained delivery of anticancer agents, *Molec. Pharm.*, **2**, 194 – 205, (2005).

18 Liu, S., Wei, X., Chu, M., Peng, J., Xu, Y.: Synthesis and characterization of iron oxide/polymer composite nanoparticles with pendent functional groups, *J. Colloids Surfaces B: Biointerfaces*, **51**, 101 – 106, (2006).

19 Tran, H.V., Tran, L.D., Nguyen, T.N.: Preparation of chitosan/magnetite composite beads and their application for removal of Pb(II) and Ni(II) from aqueous solution, *Mater. Sci. Eng. C.,* **30**, 304 – 310, (2010).

20 Shariati, S., Faraji, M., Yamini, Y., Rajabi, A.: Fe_3O_4 magnetic nanoparticles modified with sodium dodecyl sulfate for removal of safranin O dye from aqueous solutions, *Desalination*, **270**, 160 – 165, (2011).

21 Hong, R.Y., Li, J.H., Qu, J.M., Chen, L.I., Li, H.Z.: Preparation and characterization of magnetite/dextran nanocomposite used as a precursor of magnetic fluid, *Chem. Eng. J*., **150**, 572 – 80, (2009)

22 Pardoe, H., Chua-anusorn, W., St. Pierre, T.G., Dobson, J.: Structural and magnetic properties of nanoscale iron oxide particles synthesized in the presence of dextran or polyvinyl alcohol, *J. Mag. Mag. Mater.,* **225**, 41 – 46, (2001).

23 Zhai, Y., Liu, F., Zhang, Q., Gao, G.: Synthesis of magnetite nanoparticles aqueous dispersions in an ionic liquid containing acrylic acid anion, *Coll. Surf. A.,* **332**, 98 – 102, (2009).

24 Kimata, M., Nakagawa, D., Hasegawa, M.: Preparation of monodisperse magnetic particles by hydrolysis of iron alkoxide, *Powder Technol.*, **132**, 112 – 118, (2003).

25 Alvarez, G.S., Muhammed, M., Zagorodni, A.A.: Novel flow injection synthesis of iron oxide nanoparticles with narrow size distribution, *Chem. Eng. Sci.,* **61**, 4625 – 4633, (2006).

26 Basak, S., Chen, D.-R., Biswas, P.: Electrospray of ionic precursor solutions to synthesize iron oxide nanoparticles: Modified scaling law, *Chem. Eng. Sci.*, **62**, 1263 – 1268, (2007).

27 El-kharrag, R., Amin, A., Greish, Y.E.: Low-temperature synthesis of mesoporous magnetite nanoparticles, *Ceram. Int.,* submitted.

28 Atlas of Electrochemical Equilibria in Aqueous Solutions, Marcel Pourbaix, NACE International, USA, (1974).

29 Dobson, K.D., Roddick-Lanzilotta, A.D., McQuillan, A.J.: An *in situ* infrared spectroscopic investigation of adsorption of sodium dodecylsulfate and of certyltrumethylammonium bromide surfactants to TiO_2, ZrO_2, Al_2O_3, and Ta_2O_3 particle films from aqueous solutions, *Vib. Spec.*, **24**, 287 – 295, (2000)

30 Keyhanian, F., Shariati, S., Faraji, M., Hesabi, M.: Magnetite nanoparticles with surface modification for removal of methyl violet from aqueous solutions, *Arab. J. Chem.,* (2011) in press.

31 Faraji, M., Yamini, Y., Rezaee, M.: Extraction of trace amounts of mercury with sodium dodecyl sulfate-coated magnetite nanoparticles and its determination by flow injection inductively coupled plasma-optical emission spectrometry, *Talanta,* **81**, 831 – 836, (2010).

32 Zheng, W., Gao, F., Gu, H.; Magnetic polymer nanospheres with high and uniform magnetite content, *J. Mag. Mag. Mater.*, **288**, 403 – 410, (2005).

33 Rouquerol, F., Sing, K.: Adsorption by powders and porous solids: Principles, methodology and applications, Academic Press, UK, (1999).

34 Chen, R., Zhi, C., Yang, H., Bando, Y., Zhang, Z., Sugiur, N., Golberg, D.: Arsenic (V) adsorption on Fe_3O_4 nanoparticle-coated boron nitride nanotubes, *J. Colloid and Interface Sci.*, 359, 261 – 268, (2011).

35 Sahoo, Y., Pizem, H., Fried, T., Golodnitsky, D., Burstein, L., Sukenik, C.N., Markovich, G.: Alkyl phosphonate/phosphate coating on magnetite nanoparticles: a comparison with fatty acids, *Langmuir*, **17**, 7907, (2001).

36 Blum, P.: Physical Properties Handbook, Chapter 4: Magnetic susceptibility, November, (1997).

37 Si, S., Kotal, A., Mandal, T.K., Giri, S., Nakamura, H., Kohara, T.: Size-controlled synthesis of magnetite nanoparticles in the presence of polyelectrolytes, *J. Chem. Mater*., **16**, 3489 – 3496, (2004).

38 Ma, Z., Liu, H.: Synthesis and surface modification of magnetic particles for application in biotechnology and biomedicine, *J. China Particuology*, **5**, 1 – 10, (2007).